# INVESTIGATING THE INFLUENCE OF MOISTURE CONTENT AND PRESSURE ON THE BONDING MECHANISMS DURING ROLLER COMPACTION OF AN AMORPHOUS MATERIAL

James D. Osborne[1], Tim Althaus[2], Laurent Forny[2], Gerhard Niederreiter[2], Stefan Palzer[3], Michael J. Hounslow[1] & Agba D. Salman[1]

1 Department of Chemical and Biological Engineering, University of Sheffield, Mappin Street, Sheffield, S1 3JD, UK
2 Food Science and Technology Department, Nestlé Research Centre, Vers-Chez-Les-Blanc, CH-1000 Lausanne, Switzerland
3 Nestlé Product Technology Centre York, Haxby Road, York, YO91 1XY, UK
example@sheffield.ac.uk

## ABSTRACT

Roller compaction is a dry agglomeration process which uses high pressure to bond powder particles together to form an agglomerate (ribbon). The bonding that occurs depends on the compressibility, deformation and fragmentation characteristics of the material. For amorphous materials these properties vary significantly with water content. The aim of this work was to investigate the influence of water content on the physical properties of the agglomerate formed in a roller compactor.

In this work a ribbon was produced from an amorphous food polymer, dextrose syrup IT21, using a roller compactor operating at different hydraulic pressures (30-180 bar). The powder was equilibrated at different relative humidities, ($a_w$) of 0.15, 0.32 and 0.42 at 25 °C, prior to compaction. The strength of the ribbon produced was evaluated by a novel ball milling method as well as by using the three point bend test. The temperature of the ribbon was followed during production using a thermal camera.

It was found that the strength of the ribbon was dependent on both the hydraulic pressure and Tg-T value. It was shown that increasing the hydraulic pressure increases the temperature of the compacted powder up to 54 °C and this causes the material to surpass its glass transition temperature. At a certain water content and hydraulic pressure, solid bonding became the dominant bonding mechanism due to sintering of the material.

## KEYWORDS

Roller compaction, Water content, Bonding mechanism, Temperature

## 1. INTRODUCTION

Agglomeration is a size-enlargement process used to bond powder particles together to form a larger entity. It is regularly used in industries, such as food and pharmaceuticals, to improve powder properties such as flowability and uniformity as their larger size reduces cohesiveness. Industries require that these agglomerates are strong enough to survive transport to the consumer.

Roller compaction uses two counter-rotating rolls to compress powder to form an agglomerate or ‘ribbon’. The powder is usually fed to the rollers either by gravity or by means of a screw feeder. The ribbons are then passed through a milling step in order to form granules.

Roller compaction is a dry agglomeration process which means that there is no liquid addition during the process and, therefore, no need for a drying stage which can save production costs. Its other advantage over conventional wet granulation processes is that it can be run continuously, therefore increasing the efficiency of the overall process [1].

As there is no additional liquid, the particles are bonded together as a consequence of the high compaction forces acting on the material, similar to tabletting. However, the difference between roller compaction and tabletting is the magnitude of the normal and shear stresses applied to the material during processing. The type of bonding which can occur between the particles (Van der Waals forces, interlocking forces, solid bridges etc.) during agglomeration depends highly on the compressibility, deformation and fragmentation characteristics of the material [2].

Hydrophilic amorphous materials store water in their matrix structure, even if they are termed as 'dry', depending on the relative humidity of the surrounding environment. The water content of a material affects its compressibility, especially in food materials which are hygrosensitive [3,4].

In tabletting, previous work has been carried out to study the effect of water content on the compressibility of materials and the properties of the tablets formed. Li and Peck [5] and Ollet et al. [6] showed that increasing the water content affected the compression behaviour of amorphous food materials and that increasing amounts of water increased plastic deformation. Sebhatu et al. [7] supported this work by demonstrating a similar result with amorphous lactose exhibiting increasing deformability with increasing water content, therefore increasing the strength of tablets. An increase in plastic deformation will increase the bonding area between particles, therefore increasing the strength of tablets. However, Sun [8] showed that increasing amounts of water will decrease the bonding strength between particles. The final strength of the tablet was, therefore, suggested to be a trade off between bonding area; increasing with increasing water content, and bonding strength; decreasing with increasing water content [9].

One previous study to look at the effect of water content on the roller compaction process is Wu et al. [10]. Their paper investigated the effect of increasing moisture content of the powder on the behaviour of the flow of the powder through a gravity fed system. The work showed that increasing moisture contents affected the flow of powder to the rollers thereby affecting the nip angle and compaction pressure. It was suggested that at higher moisture contents the strength of the ribbons was reduced which was causing them to split at high compaction pressures. Gupta et al. [11] investigated the effect of water content on a powder blend of microcrystalline cellulose and crystalline acetaminophen. Their work showed an initial increase followed by a decrease in tensile strength with water content. This was attributed to competing effects between the mechanical properties of the two materials. The work presented in this paper will investigate the effect of water content on the strength of the amorphous ribbons and relate this to a bonding mechanism.

The water content also has an effect on the glass transition temperature of an amorphous material [4]. Close to its glass transition temperature the material moves into its rubbery state and is, therefore, much less viscous. At this point it is suggested that any contact points between powder particles may sinter together creating solid bridges [4].

These solid bridges would be stronger than any other bond holding the particles together [2] and would, therefore, produce a stronger agglomerate. Different methods have been used to assess the strength of ribbons; Gupta et al. [11] and Farber et al. [12] used a three-point bed test whilst Freitag et al. [13] used microhardness measurements. In this paper a new method is suggested which can be used for non-uniform pieces of ribbon.

The aim of this work was to investigate the influence of the water content of an amorphous material, dextrose syrup IT21, on the physical properties of the agglomerate formed in a roller compactor. It was presumed that varying the water content will affect the bonding mechanism acting between the particles, therefore affecting the strength and porosity. This was investigated by studying the relationship between the strength of the agglomerate and both the hydraulic pressure and water content separately.

## 2. EXPERIMENTAL METHOD

### Preparation of powders

Dextrose syrup IT21 (Glucidex IT21, IMCD, UK), an amorphous polymer carbohydrate, with a particle size of ~280 µm was stored in three separate relative humidities for one week to equilibrate the powder to different water activities ($a_w$) of 0.150, 0.320 and 0.422. The water activity is the vapour pressure of the water surrounding the powder divided by that of pure water at the same temperature. These were achieved using saturated salt solutions of LiCl, $MgCl_2$ and $K_2CO_3$ at 25 °C. These water activity values of the powder were determined prior to agglomerate production using Rotronic HygroLab2 with AWVC-D10 probes (Rotronic, UK).

### Ribbon production

The equilibrated powder was compressed into a ribbon using an Alexanderwerk WP120 (Alexanderwerk, Germany) roller compactor. The WP120 is a horizontally screw fed roller compactor that uses side cheeks to prevent the powder from leaking from between the rollers during compression. It is also fitted with a vacuum de-aeration system which sucks air out of the system prior to entry into the rollers and, therefore, enhances consolidation of the powder. Hydraulic pressures ranging from 30-180 bar between the 40 mm knurled rollers were used to produce a ribbon. A feedback system which constantly altered the feed rate to maintain a constant 2 mm gap between the rollers was turned on during ribbon production. The speed of the rollers was kept constant at 3 rpm throughout which resulted in a constant compression time for the material of 1 second. Cooling liquid was passed around the rollers at a constant temperature of 5 degrees throughout production. The hydraulic pressures convert to pressing force between the rollers, as shown in Table 1. This is the force applied to the powder in contact with the rollers which is the powder located in the nip region. A Flir SC 3000 thermal imaging system (ESPRC, UK) was used to capture thermal images of the ribbon as it exited the rollers.

After production, the ribbons were then stored in their prior environments before being characterised. It is worth noting that cleanly shaped ribbons were not always produced, especially at high pressures and water contents. The bulk density and porosity of the ribbons were determined from their individual mass and volume measured using a high precision balance and a digital slide calliper respectively. As well as the average ribbon porosity, the central ribbon porosity, lengthways, was also calculated by sectioning it from the outer parts. To reduce the error in the porosity calculations the average of at least ten samples was used for each pressure and water activity.

A Retsch Planetary Ball Mill PM 100 (Retsch, Leeds, UK) using a 500 ml agate jar and three 30 mm diameter balls, at 400 rpm for 30 seconds, was used to grind 5 g of ribbon. This was repeated five times for each ribbon produced at different hydraulic pressures and water contents. After milling, the size distribution of the fragments was obtained using Qicpic (Sympatec, Germany) image analysis technology.

Table 1. Conversion of hydraulic pressure to pressing force between rollers [14].

| Hydraulic Pressure (bar) | Pressing Force (kN) |
|---|---|
| 30 | 12.4 |
| 50 | 20.7 |
| 65 | 27.0 |
| 80 | 33.2 |
| 100 | 41.5 |
| 120 | 49.8 |
| 150 | 62.2 |
| 180 | 74.7 |

The tensile strength of the ribbons was assessed by using the three point bend test method and Eq. 1 [15] using a Zwick/Roell Z 0.5 materials testing machine. A fulcrum distance of 26 mm was used with the ribbon lengthways across them. At least ten ribbons were broken for each pressure and Tg-T value using a test speed of 1 mm/min.

$$\sigma_t = \frac{3.F_{max}.l}{2.b.h^2}$$

*Eq (1)*

where $\sigma_t$ is the tensile strength (Pa), $F_{max}$ is the maximum recorded force at breakage (N), l is the distance between the two fulcrums (m), b is the ribbon width and h is the ribbon thickness (m).

Electron micrographs were obtained of the ribbons using an InspectF FEI microscope (FEI Company, The Netherlands), operated at 10 kV under low vacuum conditions.

## 3. RESULTS

### Strength analysis

Figures 1, 2 and 3 show the cumulative size distributions of fragments produced at different compaction forces of ribbons after milling using powders equilibrated at different relative humidities ($a_w$ = 0.150, 0.320, 0.422 at 25 °C). The size distributions presented are the average of 5 repetitions for each measurement. It can be seen that for all the figures an increase in the production compaction force causes an increase in fragment size, with the curves shifting to the right.

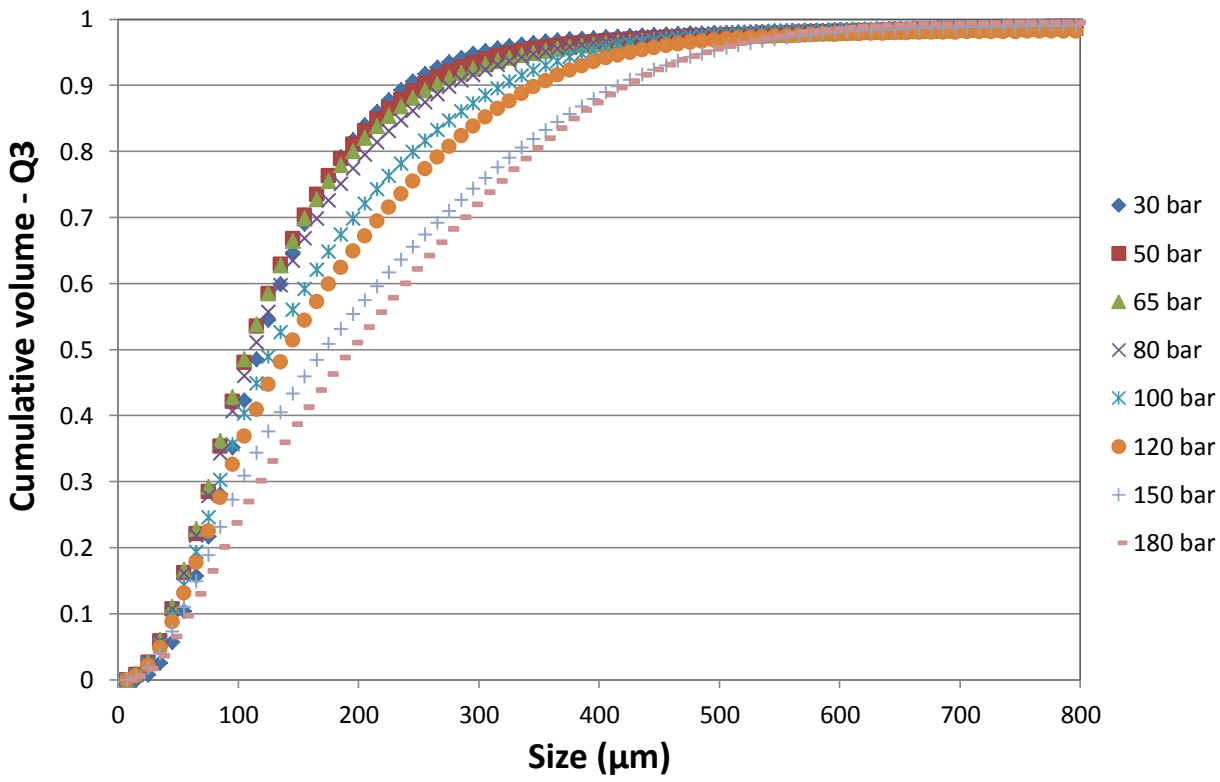


Figure 1. Cumulative size distributions of fragments of ribbon produced with powder at $a_w$=0.15 after ball milling.

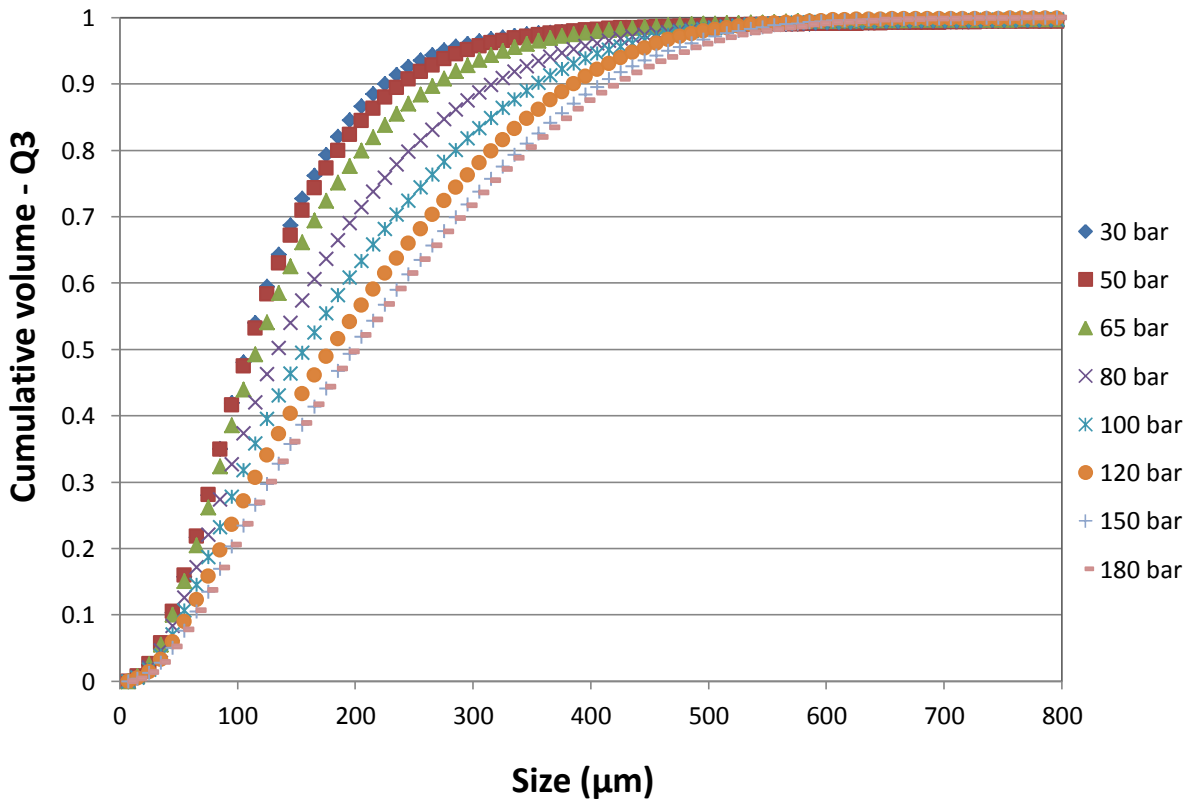


Figure 2. Cumulative size distributions of fragments of ribbon produced with powder at $a_w$=0.322 after ball milling.

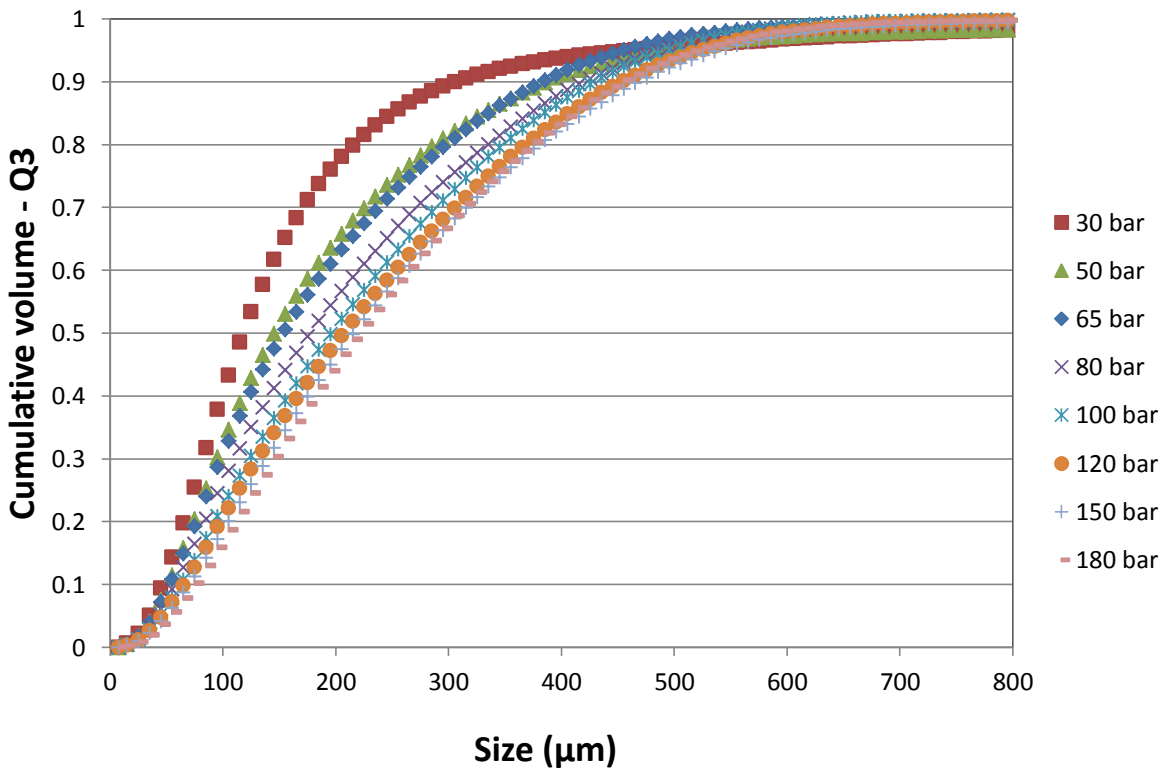


Figure 3. Cumulative size distributions of fragments of ribbon produced with powder at $a_w$=0.422 after ball milling.

From the average size distributions the $d_{10}$, $d_{50}$ and $d_{90}$ values for each pressure were obtained. Figures 4, 5 and 6 show plots of this data in terms of each of the powders' Tg-T value. The Tg-T value shows the difference between the powder's specific glass transition temperature, Tg, due to their separate water contents, and the input powder temperature before compaction, T (Table 2).

Figures 4, 5 and 6 all reiterate the fact that increasing the hydraulic pressure increases the fragment size of the ribbons after milling for all three powders. It can also be seen, that in all three figures, decreasing the Tg-T value increases the fragment size, with Tg-T=65 °C showing the smallest fragments and Tg-T=30 showing the largest fragments.

Table 2. Glass transition temperature of the powders equilibrated at different water activities [16].

| aw | Water content (%) | Tg (°C) | Tg -T (°C) |
|---|---|---|---|
| 0.150 | 4.5 | 80 | 65 |
| 0.320 | 6.2 | 60 | 45 |
| 0.422 | 7.5 | 45 | 30 |

It can be seen in Figures 4 and 5 that for Tg-T=65 °C, between 30 and 80 bar pressure there is not a significant change in the $d_{10}$ and $d_{50}$ fragment size. However, above 80 bar there is a steady increase in the fragment sizes with increasing pressure. For powder at Tg-T=45 °C, a similar trend can be seen in that at lower pressures, between 30 and 65 bar, there is little effect on the $d_{10}$ and $d_{50}$ fragment sizes. Above 65 bar pressure, similar to the Tg-T=65 °C result, there is a steady increase in fragment sizes with increasing pressure. For powder at Tg-T=30 °C, there is a steady increase in the $d_{10}$ and $d_{50}$ fragment sizes for all pressures. The gradient of the steady increase in fragment sizes with increasing pressure is similar for all three Tg-T values. Figure 6 shows that the $d_{90}$ fragment size for all three Tg-T values increases with increasing pressure for pressures below 150 bar. For higher pressures there appears to be less of an effect as the larger sizes of fragments tend not to differ.

Figure 7 shows the tensile strength data obtained from the three point bend test measurements using Eq. 1. It shows that the pressure applied to the material has a large impact on the tensile strength of the ribbons for all Tg-T values. It is shown that the tensile strength of the ribbons increases with pressure, the same result as shown using the ball milling method (Figures 4-6). However, the figure also shows that the Tg-T value of the powder appears to have little effect on the tensile strength of the ribbons. To obtain the tensile strength 10 different ribbons were used and it can be seen that there is still a relatively large amount of error in the results, especially for ribbons produced at higher pressures.

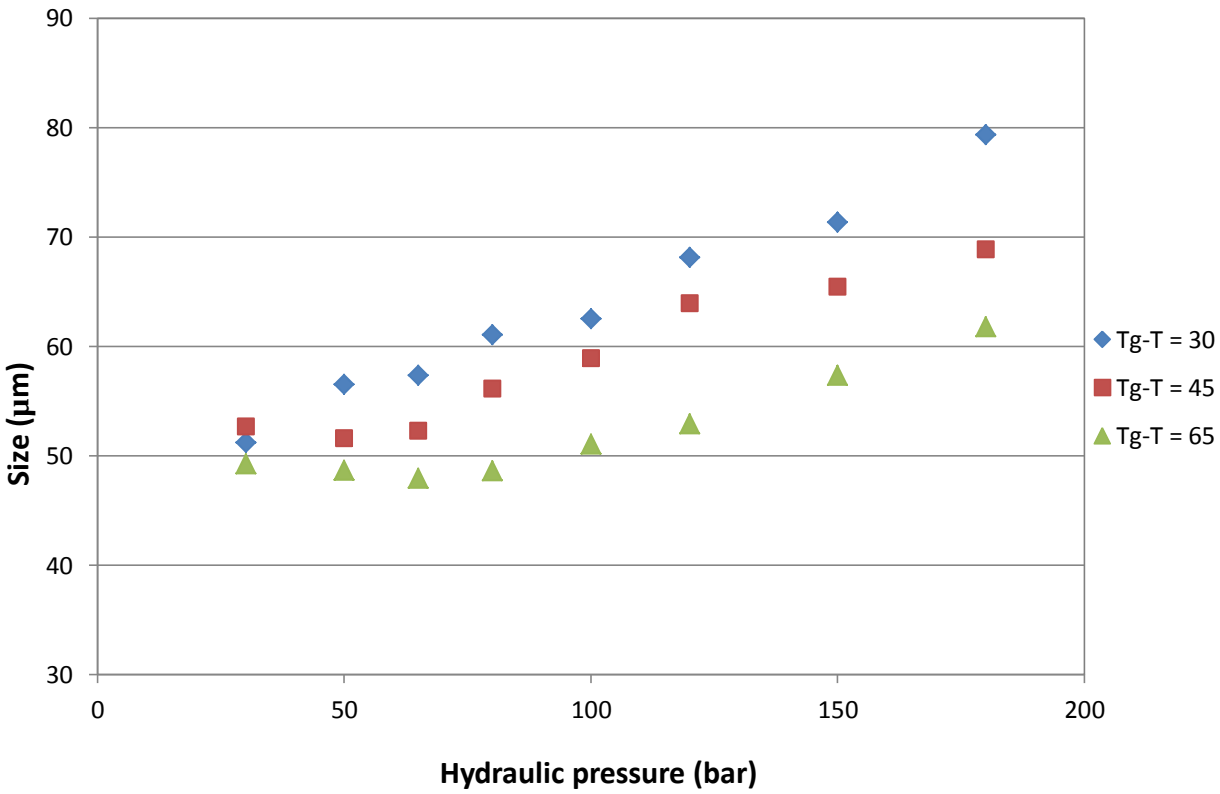


Figure 4. A plot of $d_{10}$ against hydraulic pressure for each of the Tg-T values.

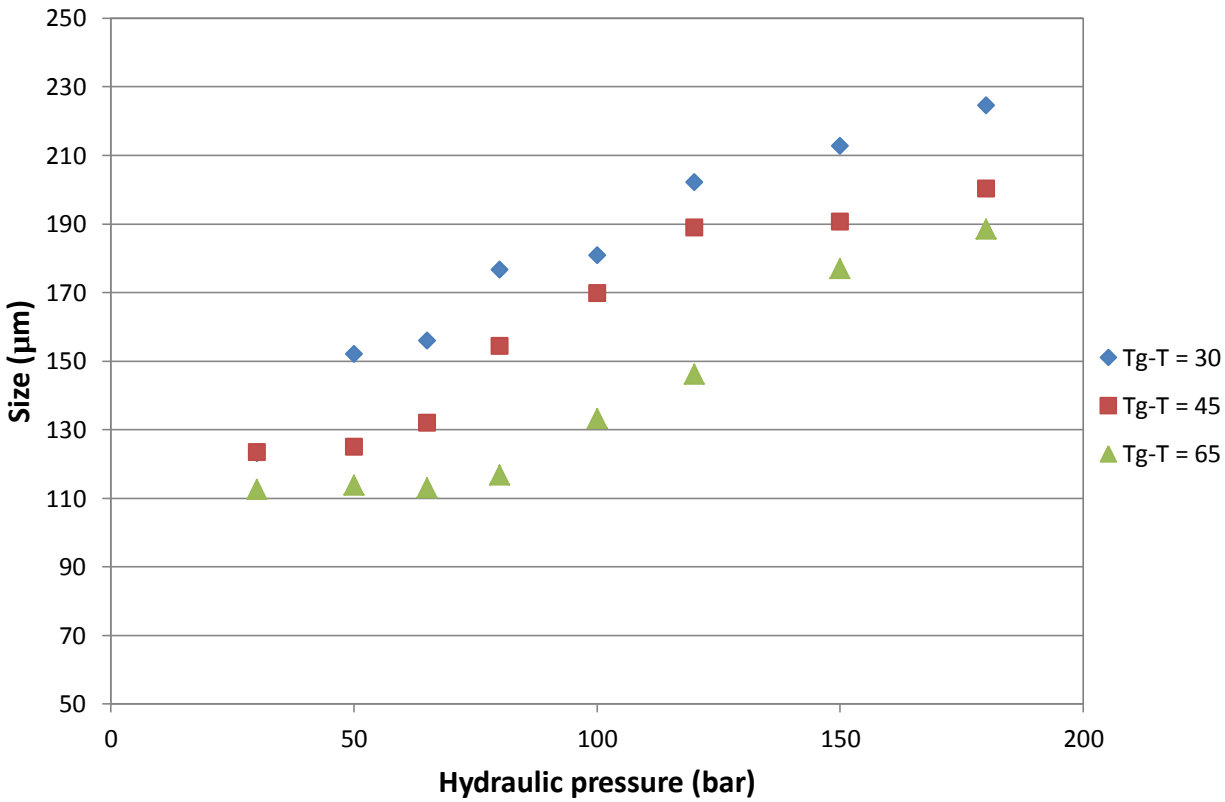


Figure 5. A plot of $d_{50}$ against hydraulic pressure for each of the Tg-T values.

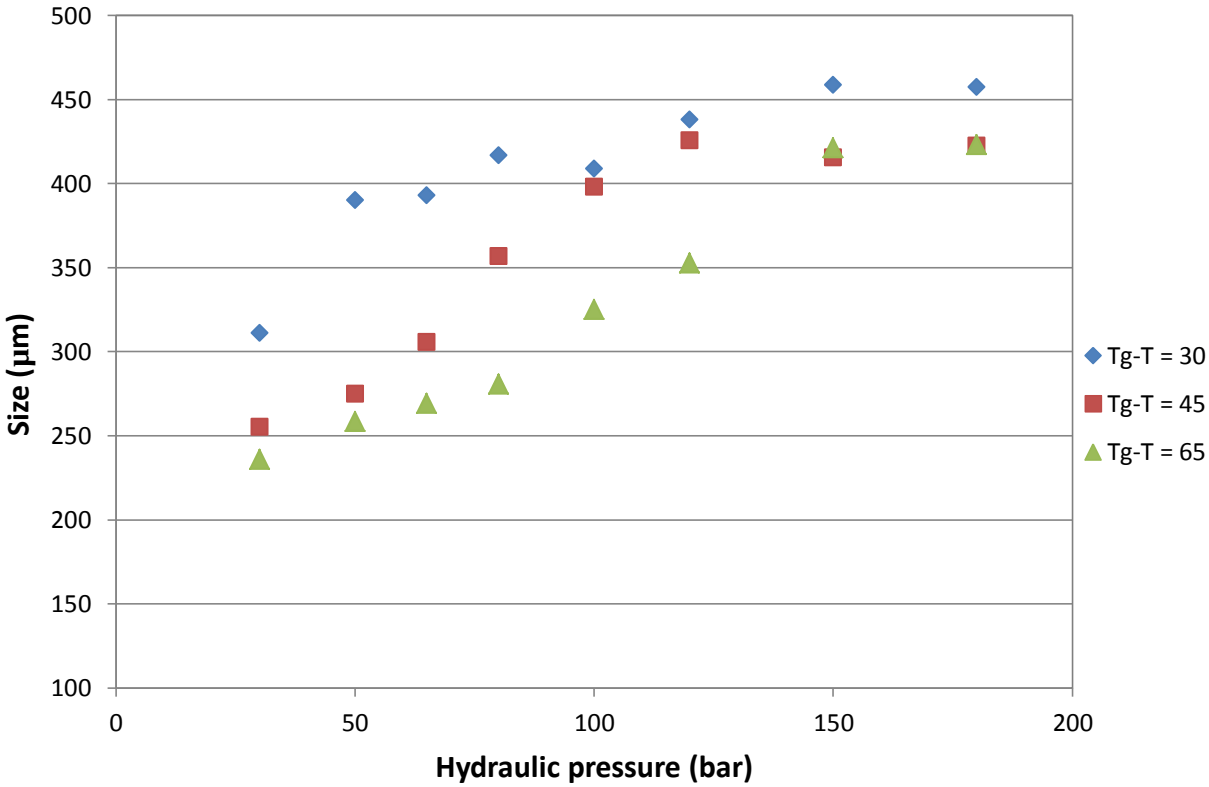


Figure 6. A plot of $d_{90}$ against hydraulic pressure for each of the Tg-T values.

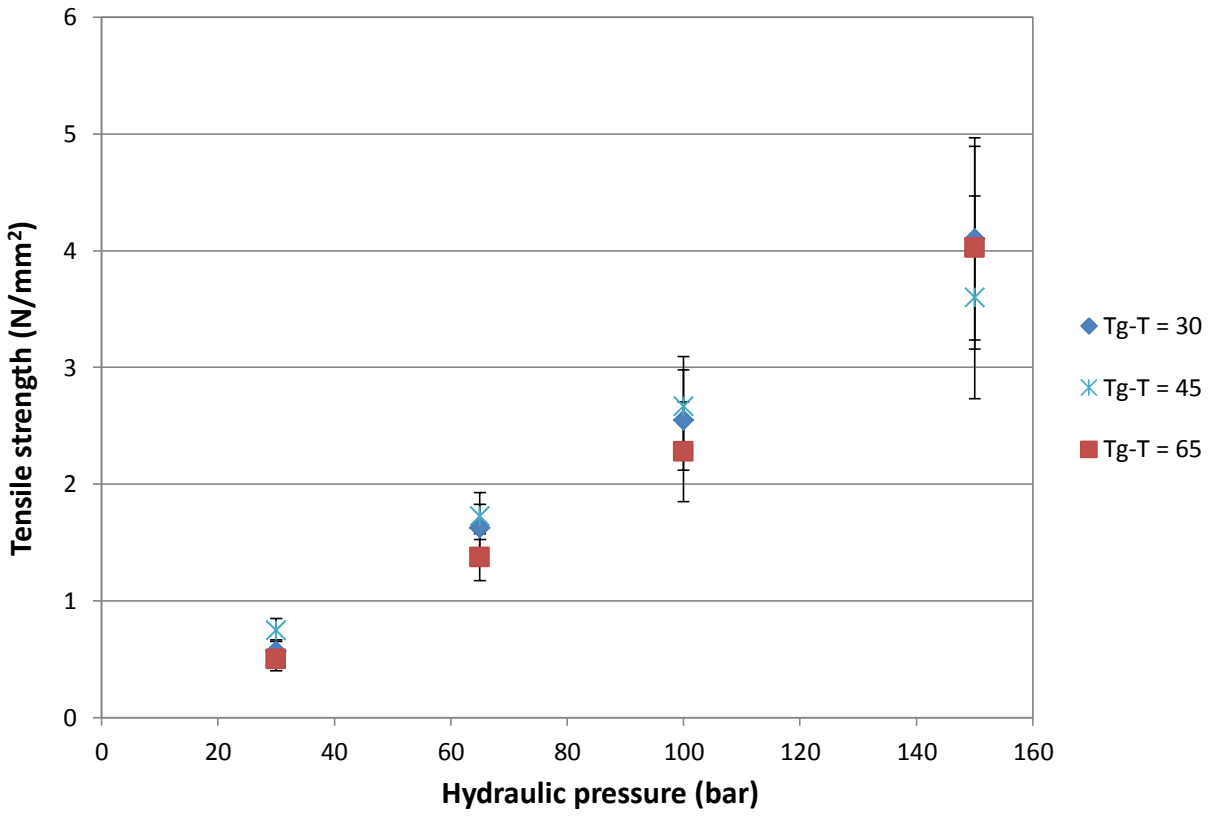


Figure 7. A plot of ribbon tensile strength against hydraulic pressure for each of the Tg-T values.

**Porosity analysis**

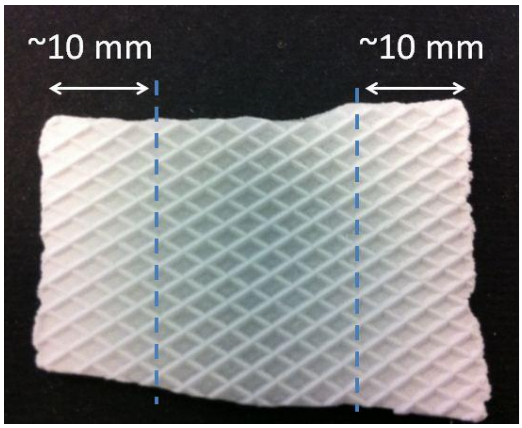


Figure 8. An image showing the method used for sectioning the ribbons.

Figure 8 shows how the ribbon was sectioned to obtain and distinguish a central porosity from the average porosity. The average ribbon and central ribbon porosity values were plotted against hydraulic pressure for different Tg-T values and are shown in Figure 9. The figure shows that increasing the hydraulic pressure decreases both the average and central ribbon porosity. It can also be seen that the central part of the ribbon is much more dense compared to the average of the whole ribbon.

The figure also shows that the Tg-T value appears to have little effect on the average porosity of the ribbons. This could be due to the standard deviation associated with the results. However, for the central ribbon porosity, a distinction between the Tg-T values can be seen, with the Tg-T=65 °C

results showing the highest porosity and Tg-T=30 °C ribbons showing the lowest porosity. At the highest pressure the porosity for all three Tg-T values becomes very similar.

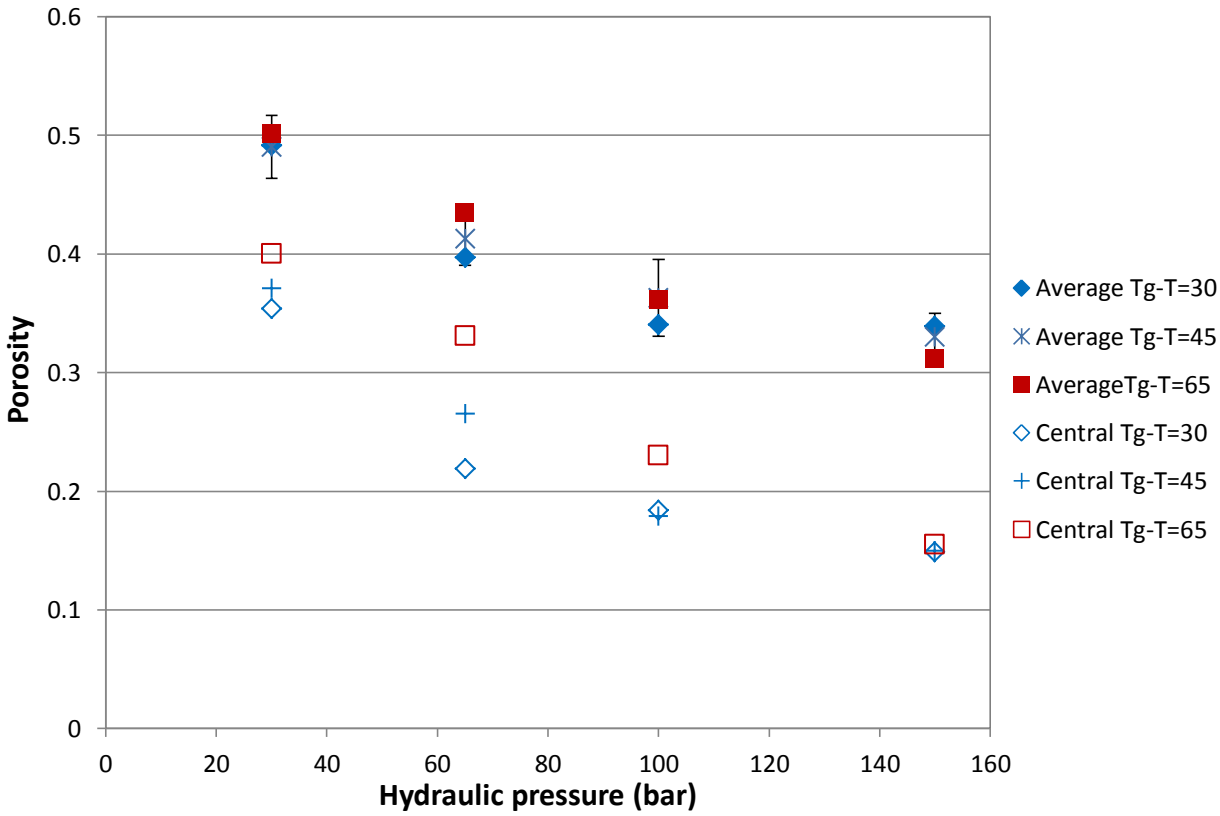


Figure 9. A plot of porosity against hydraulic pressure for each of the Tg-T values.

**Ribbon temperature**

Figure 10(a) shows a photograph of the side view of the roller compactor with the screw feeder on the left and the roller exit on the right. Figure 10(a) also shows a schematic of the setup with the thermal camera and the rollers. Three individual snapshots from the thermal imaging system of the ribbon exiting the roller compactor at different hydraulic pressures (30, 80 and 120 bar) are shown in Figure 10(b). A colour/temperature scale is shown on the right of the figure with the lighter colour signifying a higher temperature. It can be seen that parts of the ribbon appear much lighter just after exiting between the rollers at the higher pressure. In all cases, the thermal images were taken approximately 30 seconds after the feedback system on the roller compactor had reached a steady state, and a 2 mm gap between the rollers was kept constant. It can be seen from the snapshots that there is an increase in the temperature of the ribbon as it exits the roller compactor with increasing hydraulic pressure. It is worth noting that there was no increase in the temperature of the steel rollers when the hydraulic pressure was changed.

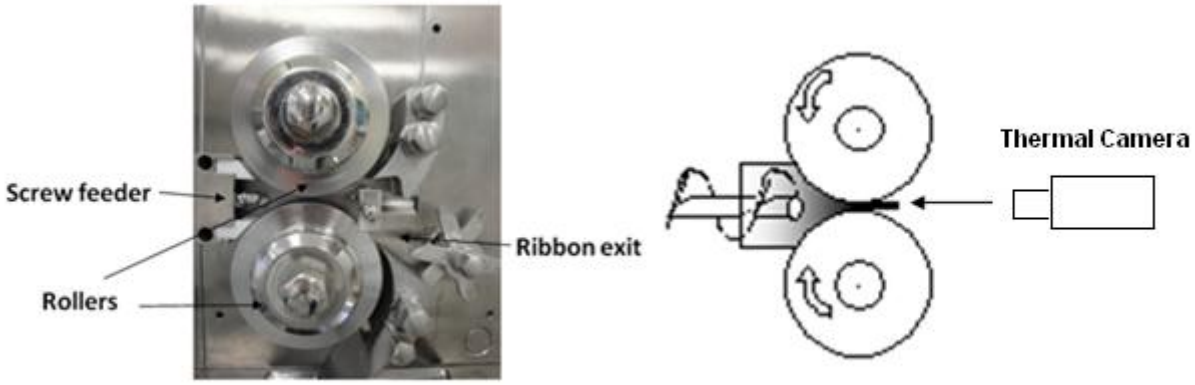


(a)

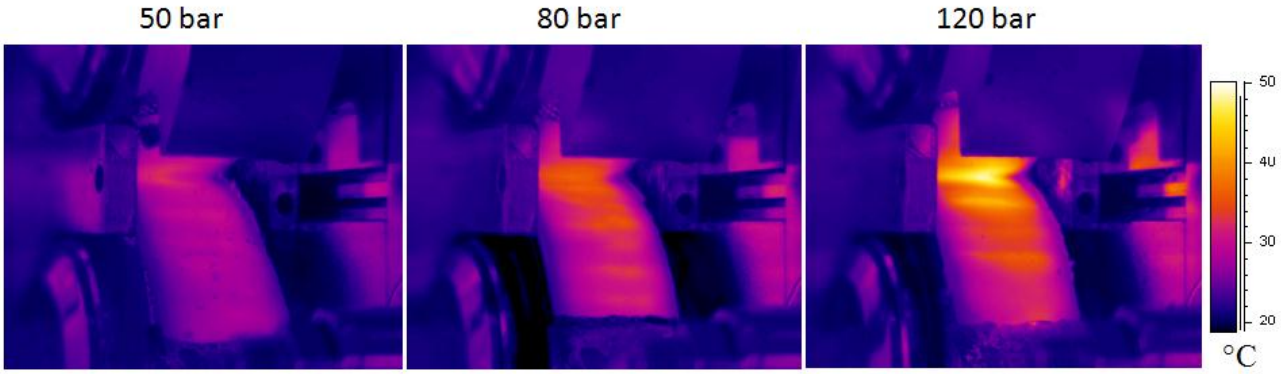


(b)

Figure 10. (a) Image showing the side view of the roller compactor (b) Image taken with the thermal camera facing the exit of the roller compactor as the ribbon is exiting at different hydraulic pressures.

This observation is reiterated in Figure 11 which shows the maximum temperature of the compacted powder seen during a ten second period of steady state production plotted against hydraulic pressure. The figure shows that there is a near linear increase in the temperature with increasing pressure. It also shows that the exit temperature of the ribbon is not affected by the Tg-T value of the powder.

## 4. DISCUSSION

### Bonding mechanisms

The results from the ball milling show that for all three powders increasing the hydraulic pressure increases the fragment size produced after milling. This increase in fragment size is an indication of an increase in resistance to breakage and, therefore, an increase in the strength of the ribbon and the bonds between the particles. This result is supported by the tensile strength data shown in Figure 7.

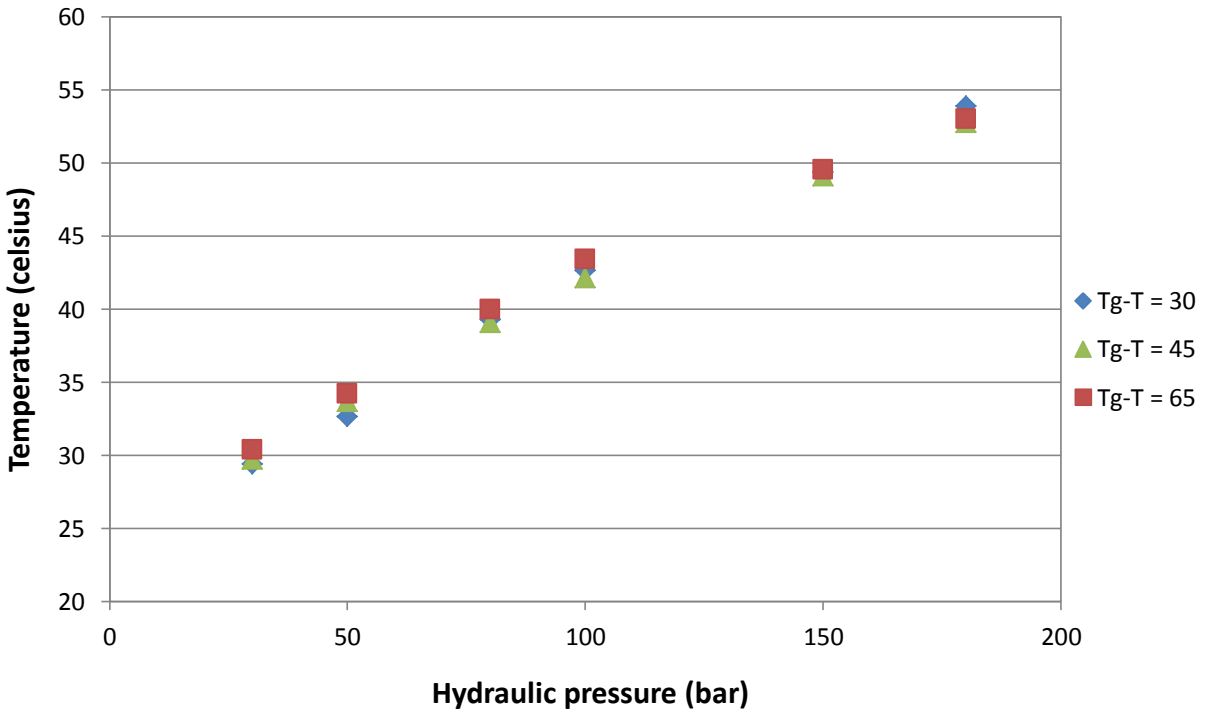


Figure 11. Ribbon temperature on exit of roller compaction using powders equilibrated to different water activities at 25°C.

It can be seen in Figure 4 and 5 that there is a degree of change between the fragment size and the hydraulic pressure between the lower and higher pressures. It is suggested that this signifies a change in the dominant bonding mechanism acting between the particles. At lower hydraulic pressures for the ribbons produced from powder with Tg-T values of 65 and 45, where the increase in strength is smaller and the ribbons are still relatively weak, it is suggested that the increase in strength is due to increased Van der Waals forces as the particles deform but do not sinter together. This is the weakest type of bonding [17] and appears to be dominant for ribbons produced at pressures around 30-50 bar for these two powders.

At hydraulic pressures above this value (>50 bar) it can be seen that for all three powders the increase in strength occurs at a higher rate. This increase in rate is suggested to be due to sintering, the creation of solid bridges between the particles as they plastically deform together. It is suggested that this sintering of material occurs when the particles are brought into contact under high pressure which causes an increase in temperature at these localised contact points [16]. The rise in temperature, caused by the high compaction forces, was captured using a thermal camera and is shown in Figure 11. It is thought that the temperatures seen are not as high as localised temperatures at particle contacts at maximum pressure, which cannot be viewed by the thermal camera.

The increase in temperature changes the mechanical properties of this amorphous material as it causes the material to become much less viscous as it surpasses its glass transition temperature and moves into its rubbery state, allowing the particles to flow into one another [4]. This allows solid bridges to form between the particles. These solid bridges then become the dominant bonding mechanism.

The increase in temperature with powder compression has been previously documented when tabletting materials [18-20], however not in roller compaction and not to this extent. Ketolainen et al. [19] showed a surface temperature increase of around 6-8 °C. It can be seen in Figure 11 that the

increase in temperature with hydraulic pressure seen with the thermal camera is independent of the Tg-T value. This explains why in the ball milling data, the lower the Tg-T value the higher the strength of the ribbon for all hydraulic pressures. This is because the lower the Tg-T value, the lower the pressure required for the powder to reach its glass transition temperature. This also explains the central porosity values in Figure 8, at lower Tg-T values a higher proportion of the particles have sintered, therefore reducing the porosity.

This result agrees with previous literature which proved that an increase in water content increased the deformation of amorphous powder during compression [6,7]. This is also supported by the SEM images which reveal the surface characteristics of the ribbons. These can be seen in Figures 12 and 13 and show ribbons produced at low, medium and high compression pressures for powders at Tg-T=30 °C and Tg-T=65 °C at different magnifications (160x and 600x).

It can be seen that there is little to distinguish between the surfaces of the ribbons produced at different Tg-T values at low pressure. However, at 80 bar pressure a difference between the two ribbons can easily be observed with the ribbon at Tg-T=30 °C appearing smoother with less particles on the surface compared to the ribbon at Tg-T=65 °C. It can also be seen that the images for the ribbon at Tg-T=65 °C at 180 bar pressure are very similar to the images shown for the ribbon at 80 bar pressure and at Tg-T=30 °C. Both show smooth surfaces which make it difficult to distinguish individual particles. This is because the amount of deformation and solid bonding is dependent on both the pressure and the water content of the powder and, therefore, Tg-T=30 °C requires less pressure to cause sintering. At 180 bar pressure for the ribbon produced with Tg-T=30 °C powder, i.e. high pressure and high water content, it can be seen that the material is almost completely flat and starts to resemble one uniform material. Furthermore, the material appears to have cracked which is likely to have happened due to unloading stresses as the ribbon exited the compactor.

These SEM images support this hypothesis that at a certain pressure, depending on the Tg-T value, the particles sinter together and solid bonding becomes the dominant bonding mechanism.

As well as a difference in surface characteristics between the ribbons, it was observed during the production of the ribbons that their appearance altered with increasing hydraulic pressure. A similar observation was made by Wu et al. [10] when increasing the moisture content of powder. It can be seen from Figure 14 that the ribbon produced at a hydraulic pressure of 30 bar with powder Tg-T=30 °C has the appearance of compressed powder. In contrast, the ribbon produced at 120 bar appears to have some parts which are translucent, looking more like a uniform solid with a smoother surface. These translucent parts appeared in the centre of the ribbon whilst the outer regions continued to look like compacted powder. This is due to a higher density in the centre of the ribbon as shown in Figure 9. At pressures above 120 bar for powder Tg-T=30 °C it could be seen that nearly the entire ribbon produced was translucent. This is due to the particles sintering together whilst in their rubbery state during compression and then moving quickly back into their glassy state.

**Strength test method comparison**

To support the results from the ball milling method the three point bend test was used to obtain the tensile strength of the ribbons. It can be seen that the tensile strength data in Figure 7 supports the ball milling data in Figures 4, 5 and 6 in that it shows the strength of the ribbons increasing with increasing hydraulic pressure.

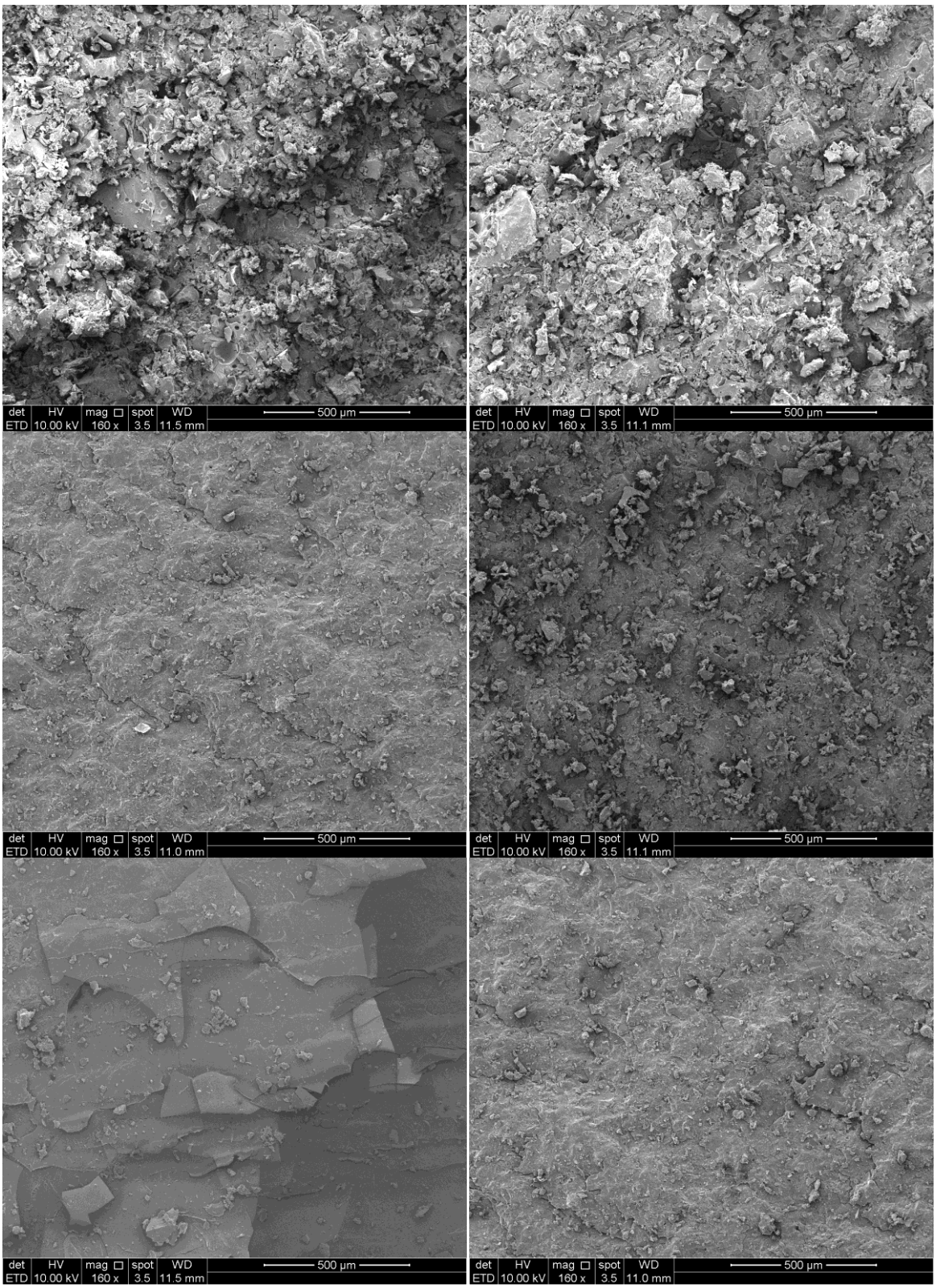


Figure 12. SEM images at 160x magnification showing the difference in structure between the ribbon produced at 30, 80 and 180 bar pressure (top, middle and bottom respectively) as well as the difference between powder at Tg-T=30 and Tg-T=65 (left and right respectively).

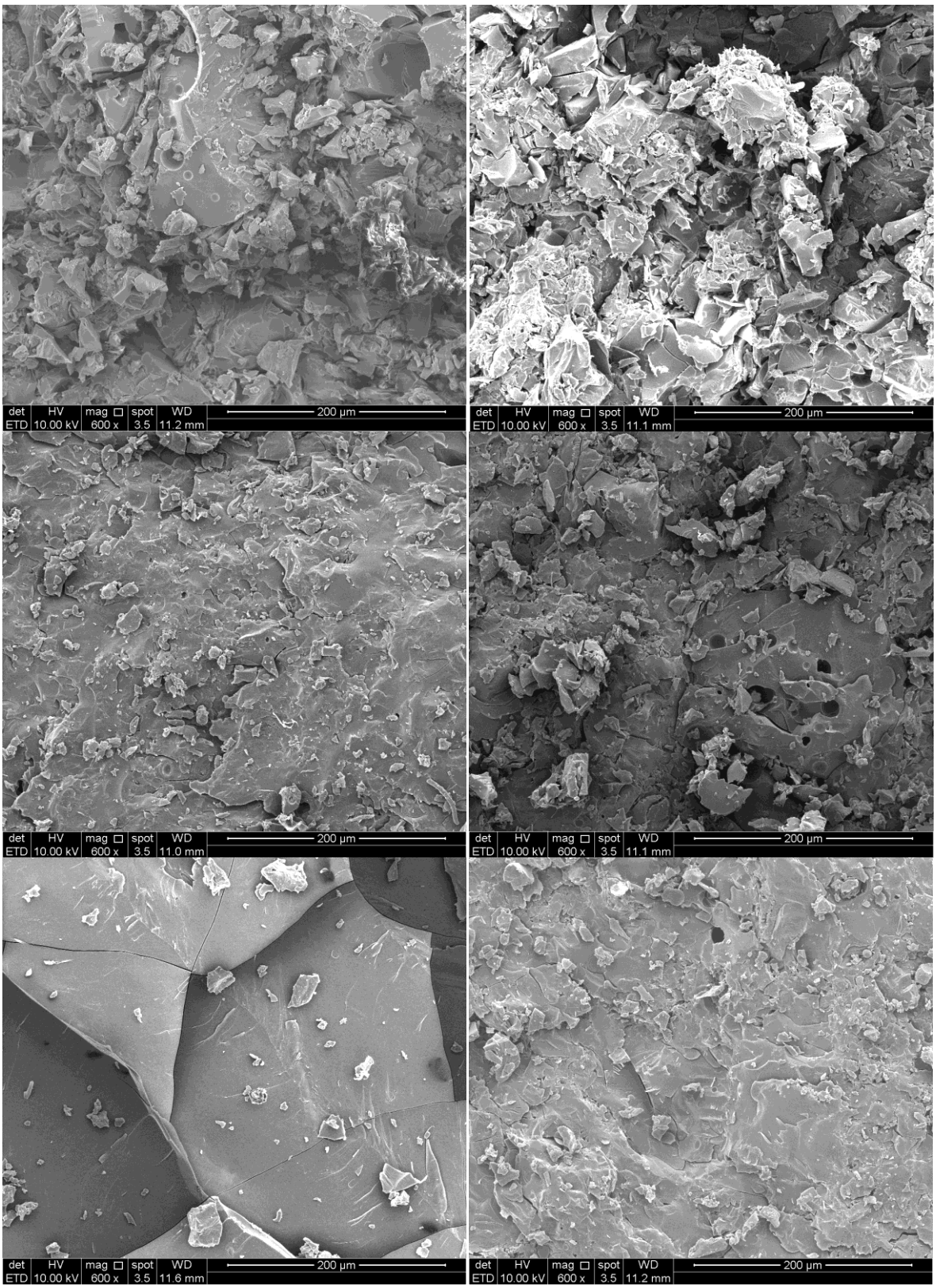


Figure 13. SEM images at 600x magnification showing the difference in structure between the ribbon produced at 30, 80 and 180 bar pressure (top, middle and bottom respectively) as well as the difference between powder at Tg-T=30 and Tg-T=65 (left and right respectively).

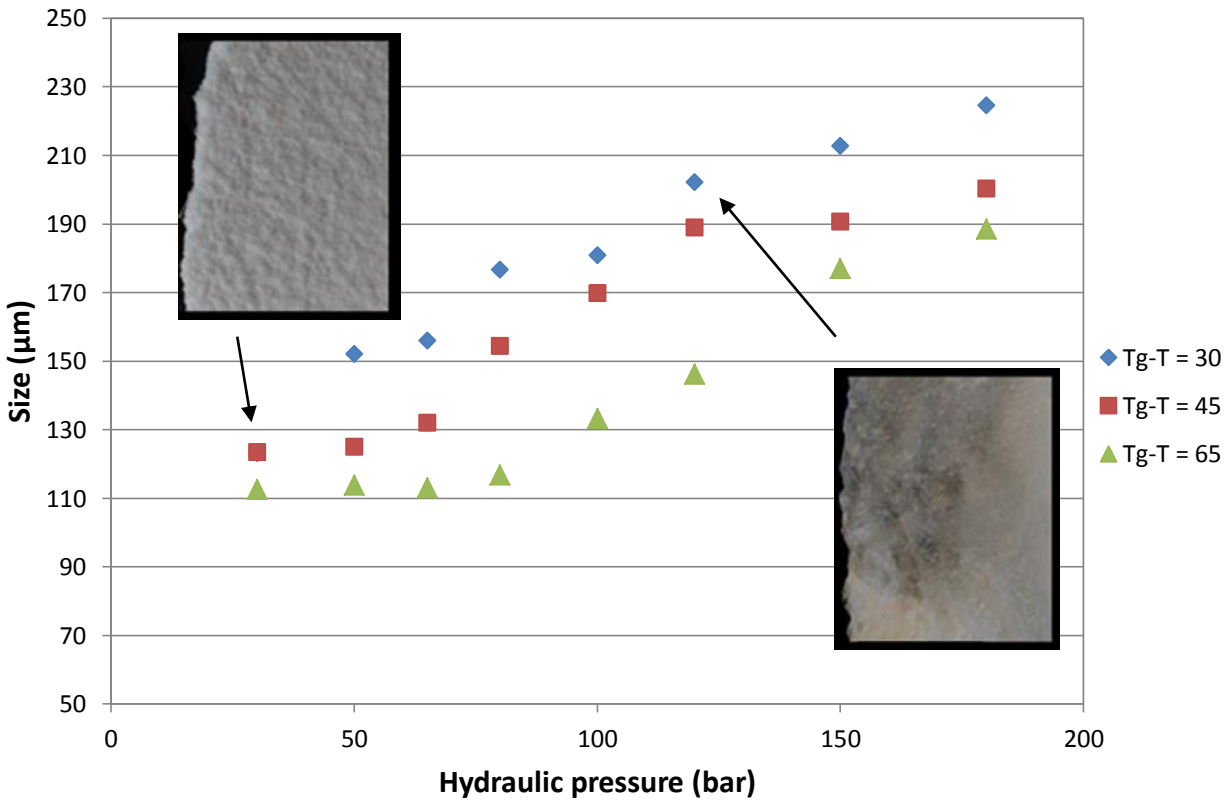


Figure 14. Optical images added to Figure 5 showing the difference in appearance of ribbon produced with powder at Tg-T=30 for different hydraulic pressures (Left: 30 bar, Right: 120bar).

However, it does not support the data when investigating the influence of the Tg-T value on the strength of the ribbons. In fact Figure 7 does not show a clear trend when comparing the Tg-T values. This is likely to be due to the error associated with this method [11] as shown by the standard error bars. The relatively large error is related to the non-uniform density across the width and the length of the ribbon, shown in Figure 9 and previous literature, which is attributable to the screw feeding system [21,22]. This also effects the average porosity measurements which show little change with varying Tg-T value. It is apparent that for this application, the ball milling method provides clearer data.

The ball milling method can also be useful when irregular shaped ribbons are produced as the shape of the ribbons is not an issue as long as the same sample mass is taken which is representative of the whole ribbon width. These ribbons cannot be tested using the conventional three point bend test. This was sometimes the case for IT21 at low Tg-T values as the material tends to stick to the rollers, even when roller cooling is turned on.

Although only the results for one material have been presented in this paper, it is put forward by the authors that any material and ribbon strength can be tested using this method. Both the rotating speed and milling time can be easily varied depending on whether more or less breakage was required to obtain a sample suitable for sizing.

Overall, the ball milling method does not give a comparable value of tensile strength; however, it has been shown that it can be used to compare ribbon strengths to investigate material and process variables especially for non-uniform density and irregular ribbons. It can therefore be used to support three point bend test data as well as for applications when the three point bend test is not possible.

## 5. CONCLUSION

This work investigated the effect of hydraulic pressure and water content on the strength and porosity of the resulting ribbons. It has shown that increasing the hydraulic pressure increases the strength of the ribbon whilst decreasing the porosity, and that it also increases the temperature of the exiting ribbon. Increasing the water content, and therefore reducing the Tg-T value, causes the central ribbon porosity to reduce whilst increasing the ribbon strength. However, the hydraulic pressure has much more of an effect overall than the water content.

Both the increasing hydraulic pressure and the water content cause more plastic deformation between the amorphous particles. This is due to a higher temperature and lower glass transition temperature respectively, which cause the materials viscosity to reduce. At a certain pressure, depending on the Tg-T value, the particles will start to sinter together as the glass transition temperature is reached and solid bonding becomes the dominant bonding mechanism.

The strength and porosity of the ribbon, produced during roller compaction of an amorphous material, is therefore dependent mainly on the hydraulic pressure but also the water content of the material. The water content of the initial material is therefore an important variable to not only consider but to be utilised in a way to control the final properties of the ribbon.

This work has also shown that the ball milling method can be used to investigate the effect of material and process variables on the strength of ribbons.

## LIST OF SYMBOLS

| | | |
|---|---|---|
| $a_w$ | Water activity | [-] |
| Tg | Glass Transition Temperature | [°C] |

## ACKNOWLEDGEMENTS

We acknowledge the use made of the Flir SC 3000 thermal imaging system which was borrowed from the EPSRC (Engineering and Physical Sciences Research Council) Engineering Instrument Pool.

## REFERENCES

[1] G. Bindhumadhavan, J.P.K. Seville, M.J. Adams, R.W. Greenwood, S. Fitzpatrick, Roll compaction of a pharmaceutical excipient: Experimental validation of rolling theory for granular solids, Chemical Engineering Science, 60 (2005) 3891-3897.

[2] H. Rumpf, Grundlagen und Methoden des Granulierens, Chemie Ingenieur Technik, 30 (1958) 144-158.

[3] A. Nokhodchi, An Overview of the Effect of Moisture on Compaction and Compression. Pharmaceutical Technology, January Edition (2005) 46-62.

[4] S. Palzer, Chapter 13 Agglomeration of dehydrated consumer foods, in: M.J. Hounslow, A.D. Salman, J.P.K. Seville (Eds.) Handbook of Powder Technology, Elsevier Science B.V., Volume 11, 1997, pp. 591-671.

[5] L.C. Li, G.E. Peck, The Effect of Moisture Content on the Compression Properties of Maltodextrins, Journal of Pharmacy and Pharmacology, 42 (1990) 272-275.

[6] A.L. Ollet, A.R. Kirby, R. Parker, A.C. Smith, A comparative study of the effects of water content on the compaction behaviour of some food materials, Powder Technology, 75 (1993) 59-65.

[7] T. Sebhatu, C. Ahlneck, G. Alderborn, The effect of moisture content on the compression and bond-formation properties of amorphous lactose particles, International Journal of Pharmaceutics, 146 (1997) 101-114.

[8] C.C. Sun, Mechanism of moisture induced variations in true density and compaction properties of microcrystalline cellulose, International Journal of Pharmaceutics, 346 (2008) 93-101.

[9] K. Van der Voort, H. Vromans, W. Groenendijk, C.F. Lerk, Effect of water on deformation and bonding of pregelatinized starch compacts, European Journal of Pharmaceutics and Biopharmaceutics, 44 (1997) 253-260.

[10] C.Y. Wu, W. L. Hung, Roller compaction of moist pharmaceutical powders, International Journal of Pharmaceutics, 391 (2010) 90-97.

[11] A. Gupta, G.E. Peck, R.W. Miller, K.R. Morris, Effect of the variation in the ambient moisture on the compaction behavior of powder undergoing roller-compaction and on the characteristics of tablets produced from the post-milled granules, Journal of Pharmaceutical Sciences, 94 (2005) 2314–2326.

[12] L. Farber, K.P. Hapgood, Unified compaction curve model for tensile strength of tablets made by roller compaction and direct compression, International Journal of Pharmaceutics, 346 (2008) 17-24.

[13] F. Freitag, K. Reincke, How do roll compaction/dry granulation affect the tableting behaviour of inorganic materials?: Microhardness of ribbons and mercury porosimetry measurements of tablets, European Journal of Pharmaceutical Sciences, 22 (2004) 325-333.

[14] Alexanderwerk, WP 120 Pharma Operating Procedure, 2010.

[15] I. Haririan, J.M. Newton, Determination of mechanical strength of same material double-layer rectangular tablets, DARU Journal of Pharmaceutical Sciences, 8 (2000) 22-27.

[16] S. Palzer, Influence of material properties on the agglomeration of water-soluble amorphous particles, Powder Technology, 189 (2009) 318-326.

[17] C. Nystrom, G.R. Alderborn, Bonding Surface area and Bonding Mechanism-Two Important Factors for the Understanding of Powder Comparability, Drug Development and Industrial Pharmacy, 19 (1993) 2143-2196.

[18] E.J. Hanus, L.D. King, Thermodynamic effects in the compression of solids, Journal of Pharmaceutical Sciences, 57 (1968) 677-684.

[19] J. Ketolainen, J. Ilkka, Temperature changes during tabletting measured using infrared thermoviewer, International Journal of Pharmaceutics, 92 (1993) 157-166.

[20] D.E. Wurster, C.E. Rowlings, J.R. Creekmore, Calorimetric analysis of powder compression: I. Design and development of a compression calorimeter, International Journal of Pharmaceutics, 116 (1995) 179-189.

[21] A.M. Miguélez-Morán, C-Y. Wu, Characterisation of density distributions in roller-compacted ribbons using micro-indentation and X-ray micro-computed tomography, European Journal of Pharmaceutics and Biopharmaceutics, 72 (2009) 173-182.

[22] A. Michrafy, H. Diarra, Experimental and numerical analyses of homogeneity over strip width in roll compaction, Powder Technology, 206 (2011) 154-160.